




# Development of a Novel High Temperature Continuous Particle Mass Flow Measurement Device for Particle-Based CSP Applications

Hendrik Frederik Laubscher<sup>1</sup>, Samuel C. Hastings<sup>1</sup>, Kaden E. Plewe<sup>1</sup>, and Luke P. McLaughlin<sup>1</sup>

<sup>1</sup> Sandia National Laboratories, USA

\*Correspondence: Hendrik Frederik Laubscher, [hlaubsc@sandia.gov](mailto:hlaubsc@sandia.gov)

**Abstract.** Particle-based concentrating solar power (CSP) technology is one of the generation three (Gen3) CSP technologies that has potential for lowering the levelized cost of electricity produced by this solar thermal power systems. Commercially available ceramic particles, which are rated for high temperature applications up to 1200 °C, were selected for this study. This medium is commonly used as an energy carrier or heat transfer medium in Gen3 CSP research and development efforts [1]. Prior studies at the National Solar Thermal Test Facility (NSTTF) have investigated and evaluated various mass flow measurement methods, and a simple gravimetric temporal load measurement method was chosen as the best candidate for the research purpose [2]. This mass flow measurement method is a batch process and is not a viable solution for commercial-scale power generation applications based on cost, space, process control, and practical system integration factors. In-line and continuous particle mass flow measurement will play an integral role in efficient and cost effective Gen3 CSP particle technologies. Process parameters, including energy absorbed by the particles, receiver efficiency, temperature dependent flow phenomena, and general high temperature measurement reliability are all rely on repeatable and accurate measurement of particle mass flow under various operating conditions. Ceramic particles, like those used in this application, are not conventionally used as an energy carrier. A novel concept for continuous particle mass flow at a wide range of operating temperatures is currently under development and planned to be tested at the NSTTF, called the Particle In-LinE (PILE) mass flow sensor.

**Keywords:** Particle-based CSP, Particle Mass Flow Measurement, High Temperature Particle Flow

## 1. Introduction

The concept for continuous mass flow measurement of particles at high temperature is described in this paper. In-line and continuous particle mass flow measurement is critical in the process controls methods for efficient and cost effective Gen3 CSP particle technologies. A simplified design based on a material retention principle is investigated in this study and proofed to be a practical solution for use in harsh operating environments. Experimental design, concept generation of various engineering solutions and preliminary experimental results are described here. A few practical lessons learnt that will influence future design for larger scale applications have been identified and pathways to proceed are defined. Since the current state-of-the-art method used in research and development for measuring high temperature particle mass flow rates is based on a simple gravimetric method, a need for reliable in-line

continuous mass flow measurement is clear. Gravimetric measurement is typically done in a batch flow fashion, which result in intentional disruption in the particle flow stream [2]. However the batch flow regime can be tolerated in experimental design for research purposes, utility scale applications would not implement this batch measurement method. It would be too costly, constrained on available space and unable to provide real time mass flow measurement for use as feedback signal to a process control system.

## 2. First Generation Design

### 2.1 Mass Flow Sensor Working Principle

The basic working principle of the proposed particle mass flow device is analogous to that of a traditional water weir. A cylindrical bucket, open at the top, has a slot in the side (or multiple). As particles fall into the cup from above, they spill out the side of the cup. The overflow level of particles through the slot in the flow bin is proportional to the overall volumetric flow going through the measurement device. Due to the nature of gravity driven granular flow of sub-millimeter particles, the level in the flow bin will not be as representative of the actual inventory in comparison with a liquid fluid, such as water. Therefore, the instantaneous mass of the flow bin, measured by a load cell, will provide a better indication of the inventory at a point in time. The approximate level of particles in the bin correlates to the height of particle overflow. The higher the level, the more particle overflow will take place, thus higher particle mass flow rates can be continuously maintained. This will produce a steady reading at a pseudo steady state, when the inlet and outlet flow rates match. The load cell will also be measuring forces from the impact of the particle flow into the bin, but this effect can be minimized by locating the bin as close to the feed aperture as possible.

In CSP, particles in a system are kept at very high temperatures. Due to this, the load cell in the device will not be able to function if it is placed in proximity to the flow bin. Figure 1 shows a concept design of the device. An arm with a hinge allows the flow bin to be positioned at some distance from the load cell, raising the operating temperature of the sensor to accommodate extremely high-temperature particles, potentially up to 800 °C. The lever arm will increase the sensitivity of the sensor because it will act as a load amplifier, but it will also increase the noise in measurement. Therefore, it is important to be strategic about the location of the load cell along the arm.

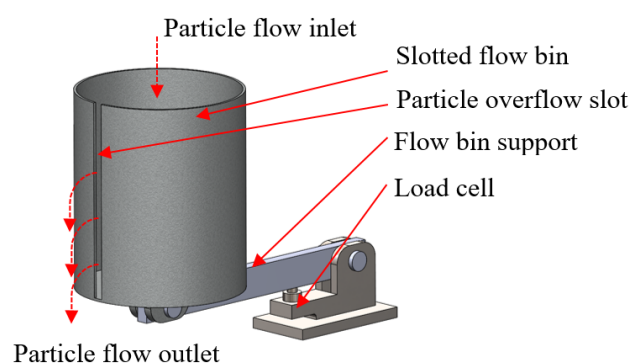


**Figure 1.** Labelled concept of mass flow rate sensor.

For the sensor to be useful in particle-based CSP, it needs to be able to provide adequate information of the flow rate to be able to be used for real-time flow control. This requires continuous measurement, repeatable and repeatedly accurate results, and robust design and construction for functionality in extremely harsh environments. In commercial applications, the sensor will be under constant high-temperature and high-volume particle flow at all times of facility operation. In certain locations, a sensor will be subjected to heating and cooling multiple

times during a daily operating cycle. A small-scale prototype is designed to test the viability of the concept of mass flow rate measurement at high temperature.

## 2.2 Concept Generation

The viability of the in-line mass flow rate sensor is dependent on its ability to repeatedly deliver accurate results, and on its ability to be used in a variety of situations within a particle-based CSP system. Generating a working prototype to demonstrate the concept of a flow meter for high temperatures has multiple considerations.

High temperature use constitutes the use of high quality material to avoid corrosion. Stainless steel is the material of choice for this sensor because it will not degrade due to the temperature of the particles in the system. To optimize the flow bin, testing different configurations is essential. Therefore, an interface between the lever arm and the flow bin that allows for replacement of the bin is implemented. Due to high heat and submillimeter particles, the interface requires simplicity and robustness. In the test facility that is available, space for the sensor is extremely limited. The sensor design is tailored to be integrated into a limited area, which requires precision in design, manufacturing, and installation. The scale of the prototype and test facility are much smaller than potential future applications, and prototype design must be scalable to accommodate much larger flow rates. Overall, prototype cost must be minimized to demonstrate the sensor's economic feasibility in commercial applications.

### 2.2.1 Concept One

The first prototype assembly is designed and a CAD model created in SolidWorks with estimated measurements of the test environment. This is used to simulate the mechanical and thermal abilities of the sensor. Figure 2 shows the full layout of the assembly. Simulations are utilized to assess design performance, highlight weak points in the system, and contribute to a more robust prototype.

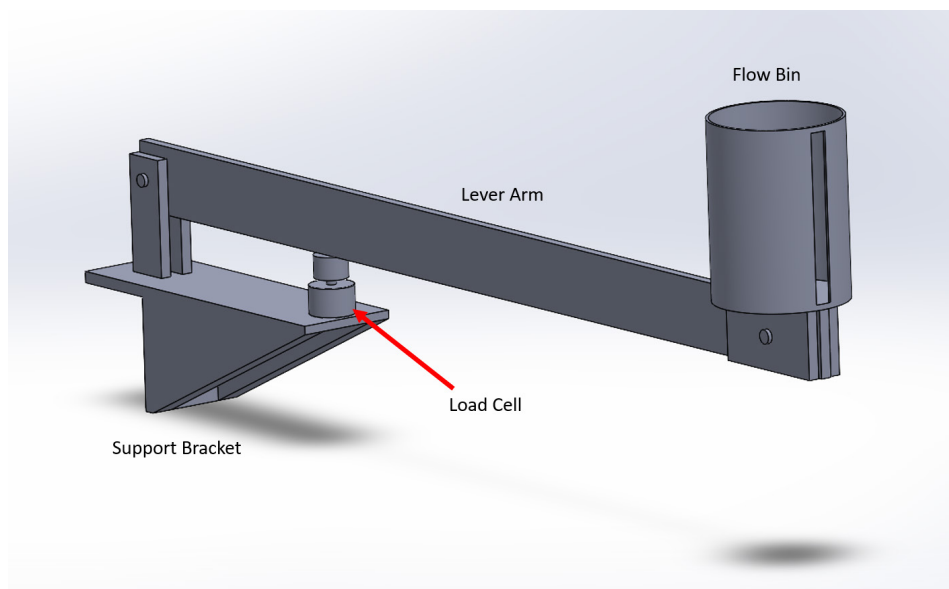


**Figure 2.** Initial prototype model, relevant parts are labelled.

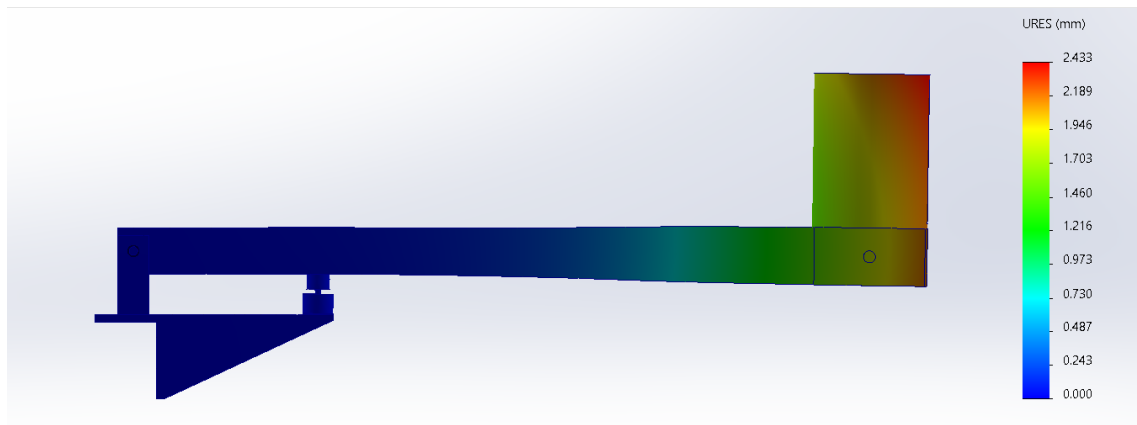


**Figure 3.** SolidWorks simulation where an external load of 5 lbs. is applied to represent the weight of the particles, the force of gravity is applied, and a worst-case temperature scenario is applied, in which 600 °C temperatures are applied to the bin and 8 inches of the beam – the “hot zone”.

Multiple types of simulations are described: static studies, thermal studies, and the combination of the two. Static studies are based on calculated external forces on the sensor. The thermal study on this model investigates a worst-case scenario where an entire third of the lever arm is exposed to a 600 °C condition. The combination looks at the displacement of the sensor at those high temperatures. Figure 3 shows the simulated deformation of the model underestimated near-maximum loading and temperature conditions. At worst, the bin might experience a maximum deformation of over 2 mm at high temperature conditions. This is less than 0.5% elongation over the length of the beam and will not affect the flow bin’s function. However, there are other simulation results that show issues with the design. Table 1 details the different simulations conducted and explains the results.

### 2.2.2 Concept Two

The results of model simulations show that the sensor needs a measure to prevent excessive stress within the load cell. A ball bearing is chosen to do so because it transfers only one-directional force to a flat surface. A clamp is also added to hold the ball bearing so that the location of the ball bearing can be manually moved to the correct location. This combination ensures that the force that is being transferred is purely in-line with the load cell, and is implemented in the model shown in Figure 4, which is the design of the manufactured prototype that is tested. Other changes from the original model are the flow bin-beam interface and the bracket design, which were changed during manufacturing based on available materials. The most important difference is that the load cell is on the other side of the beam, which is done to accommodate the limited amount of testing space that is available. This configuration of the sensor is set up specifically for the testing facility, and will be changed for different scenarios as necessary. However, it demonstrates the versatility of the sensor.

**Table 1.** Simulation descriptions and results.

Simulation Type	Performance Metric	Setup	Results
Thermal	Temperature	600° C temperature is applied in the hot zone	Temperature at load cell is well within operating range, so load cell is in a good position
Static	Stress (von Mises)	5 lb load is applied where particles will be, and gravity force is applied to make simulation more realistic	Stress inside load cell reaches 76 MPa, which is far higher than acceptable. (Simulation material yield strength is 172 MPa) Other components are at relatively low stress.
Static	Displacement	5 lb load is applied where particles will be, and gravity force is applied to make simulation more realistic	Maximum displacement in system is 0.227 mm. This amount of deformation is acceptable.
Static+ Thermal	Stress (von Mises)	Same external loads as static test, with thermal effects from thermal study applied as well.	Maximum stress in the load cell is 97 MPa, even higher than non-thermal test. Other components are at relatively low stress.
Static+ Thermal	Displacement	Same external loads as static test, with thermal effects from thermal study applied as well.	Maximum displacement due to thermal expansion and load is 2.433 mm. This amount of displacement is still acceptable
Static+ Thermal	Factor of Safety	Same external loads as static test, with thermal effects from thermal study applied as well.	Factor of safety in some components is less than two. This model needs additional measures to improve performance.

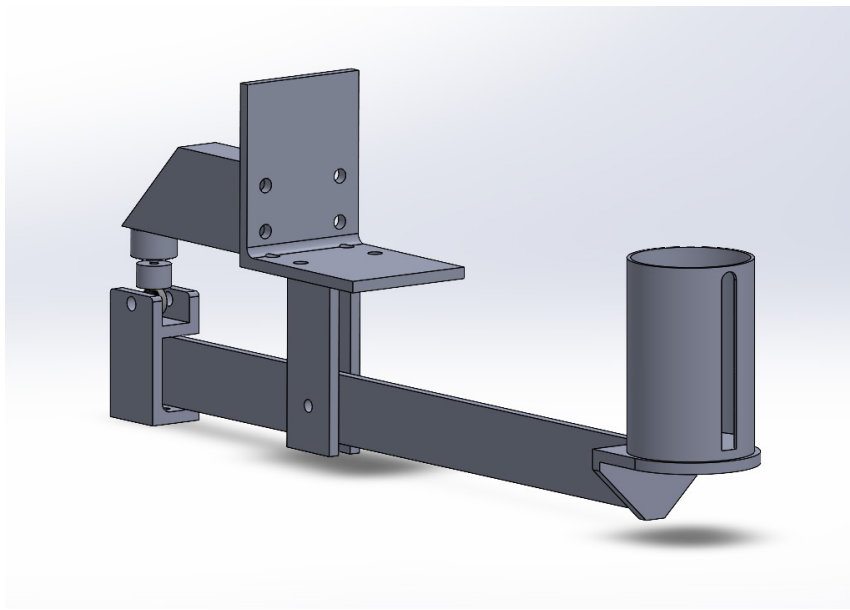


**Figure 4.** SolidWorks assembly of manufactured sensor.

The load cell that is procured is an Omega Engineering LCFD-100 load cell. It is rated at loads up to 100 lbs (~45 kg), with a safe overload capacity of 150%. Based on the liberal estimation that the weight of particles in the flow bin will be less 5 lbs (2.27 kg) at maximum, and the

weight of the beam and the other components, the force on the load cell is calculated to be 20 lbs (~9 kg) at more-than-maximum flow conditions. Cross-loading of the load cell is accounted for due to the addition of the ball bearing, which is an SKF 628/8-2RS1 ball bearing rated for static linear loading of over 100 lbs (45 kg). The model has a factor of safety of more than 5 at loads exceeding capacity of the sensor, so it is chosen for manufacturing and testing. Concept two described in Figure 4 is the design and geometry that was used for experimental testing in this study.

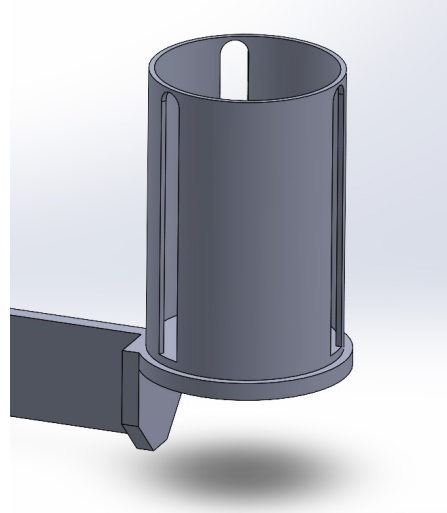


Figure 5. Slotted flow bin with 3 slots.

### 2.2.3 Concept Three

For higher flow rates, the slotted flow bin can be adapted. At the prototype scale, flow rate can be increased by increasing the area of slots in the flow bin – the “flow area”. Intuitively, increasing the area through which particles can flow will increase the flow rate capacity in the flow bin. This can be done in multiple ways: increasing the height of the bin, increasing the slot width, and increasing the number of slots contained by the bin. Figure 5 shows a model slotted flow bin with 3 slots, which has triple the flow area of the bin in Figure 4. Alternatively, differently shaped slots can increase the flow area. Triangular-shaped slots that widen with height could be utilized to allow for higher sensitivity at low flow rates but large total flow capacity.

That flow rate and flow area are proportional is a clear correlation. However, are they proportional? The mass flow rate of particulate solids through vertical slots is examined thoroughly in literature, and some analytical equations have been derived. The Beverloo equation and its subsequent variations are commonly used to predict particle flow through slots and holes describe a form of the Beverloo equation that is used to predict particle flow through a circular orifice at the bottom of a hopper or silo [3]:

$$\dot{m} = C\rho g^{\frac{1}{2}}(D - kd_p)^{n+\frac{1}{2}} \quad (1)$$

In equation (1),  $\dot{m}$  is the mass flow rate,  $C$  is a dimensionless constant related to material properties,  $\rho$  is the bulk density of particles,  $g$  is the acceleration due to gravity,  $D$  is the diameter of the hole,  $k$  is a dimensionless constant that accounts for the effective outpouring diameter being smaller than the actual orifice area, and  $d_p$  is the particle diameter. These constants were derived from experimental data in previous studies [4]. For 3-dimensional cases,  $n=2$  [3]. Harris et al. use the Beverloo equation coincidentally with their own analysis of particles flowing from vertical slots, and provide the following equation [5]:



$$\dot{m} = Cg^{\frac{1}{2}}\rho h(W - kd_p)^{\frac{3}{2}} \quad (2)$$

In equation (2),  $h$  is the active slot height and  $W$  is the slot width. Based on this equation, it is easy to see how mass flow rate through one slot relates to flow area. Assuming a much larger slot width than particle diameter ( $W \gg d_p$ ), the following relation becomes apparent:

$$\dot{m} \propto hW^{\frac{3}{2}} \quad (3)$$

Equation (3) explains multiple things. First, it shows analytically that flow rate is directly proportional to the active slot height, which supports that mass flow rate can be correlated with the weight of the flow bin. Equation (3) also provides insight into the scalability of mass flow rate sensors; knowing that flow rate can be increased more by slot width changes than by slot height increases will allow for more efficient design.

## 2.2.4 Proposed Design for Commercial Scale

In commercial facilities that employ this technology, additional features may be desired or necessary to support large quantities of particle flow and to provide robustness and reliability. Figure 6 is a CAD representation of a possible sensor conceptual layout that is developed to fit in-line with a particle-based concentrated solar power facility. This design contains four arms with four load cells, allowing for much higher stability and measurement range. However, four load cells may decrease sensitivity and increase uncertainty. In commercial applications, the configuration of the sensor may be adjusted to fit specific needs. The prototype is an example that shows that adjusting the sensor to fit different situations is possible.

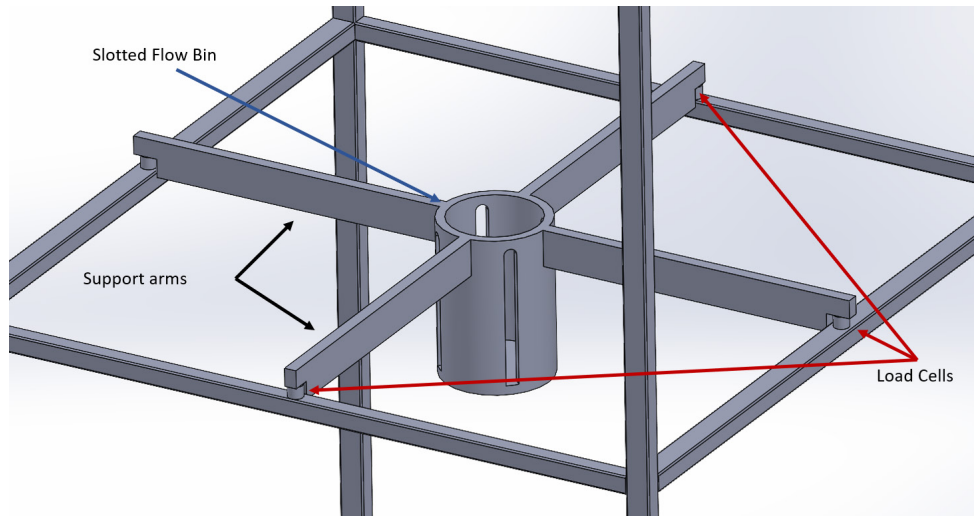


Figure 6. Theoretical model of large-scale mass flow rate sensor.

## 3. Experimental Design and Testing Details

### 3.1 System Summary

The facility that was used to test is an existing particle circulation facility which contains a 15-foot-tall structure. This system has a particle lift to transport particles to the top, a particle heater, a heat exchanger, and a weigh hopper at the bottom. The facility had no additional vertical space for the installation of the sensor, so the sensor was installed to the frame in a location where the flow bin sat inside of the lower weigh hopper. This positioned the flow bin directly under a slide-gate, which could open and close to set positions to control the particle flow. This allowed for direct control of particle flow, and immediate flow measurement. The

particles were to flow through the slide-gate aperture and the flow bin, and to collect in the weigh hopper. This setup would provide mass measurement from the sensor, and the weigh hopper would provide the calibration data that was required to calibrate the sensor.

The goal for testing was to calibrate the prototype so that the mass reading from the load cell gives information on the flow rate. Continuous mass is recorded from the sensor, and to give the calibration information, the hopper into which particles flow after the sensor has a mass recording. The mass flow rate is derived from the hopper mass, which accumulates over time, allowing for the calculation of mass over time to give a flow rate. It is this flow rate which will be used to calibrate the sensor mass reading. For the test, the slide-gate was set, and particles flowed through the sensor and into the weigh hopper. Once the weigh hopper reached capacity, it dumped its particles, and began to fill again. This process was repeated at different slide-gate positions to gather data on the full range of flow rates. For each slide-gate position, the particles were flowed for three cycles of weigh hopper filling. This allowed for lots of continuous data at each flow rate. For the higher flow rates, data had to be gathered in intervals, where the flow rate was paused momentarily to allow the particle lift to cycle fully. This is because the particle lift cycle time was longer than the time that it took for the weigh hopper to fill at the highest flow rates.

The facility that was used to test the sensor prototype has multiple things that introduced fluctuation in the data. The particle lift mechanism introduced noise into the system, as well as momentary errors in force reading when the particle lift reached the top and bottom of the system. The errors were due to the particle lift stopping, putting a force on the frame which was picked up by the load cell. Aside from this error, the signal noise from the particle lift movement was random, but there was too much amplitude for the data to be useful. Another source of potential fluctuation was from the fluidization of the particles which took place above the sensor. The heat-exchanger that was installed in the facility required particle fluidization in order to flow particles through at high rates. The flow rate was affected by changes in the fluidization, meaning that the fluidization had to be carefully controlled to provide a consistent flow rate. Even with close monitoring, however, the fluidization most likely introduced small random flow fluctuations.

### **3.2 Data Acquisition**

Data recording was done using LabVIEW software. The sensor load cell provided a voltage signal, which was correlated to a mass measurement. The measurements of relevant data in the system were done with current signals. The most important system data were the weigh hopper mass and the slide-gate position. LabVIEW was also used to control the system components including the slide-gate position, particle lift, and fluidization.

### **3.3 Preliminary Results**

Preliminary results are provided in Figure 7 below on the initial experimental testing and calibration. The reference values that are obtained from a gravimetric method are correlated with the mass of the load cell reading from the experimental setup. The sensitivity of the flow sensor is defined as mass flow relative to the output signal. A typical output signal in mA will yield the units of kg/s per mA, which is obtained for each unique flow meter. The uncertainty analysis for the measurements and calibration accounted for load cell uncertainty, measurement precision, and calibration error and follows the suggested Nth-Order uncertainty analysis procedure suggested in [6].



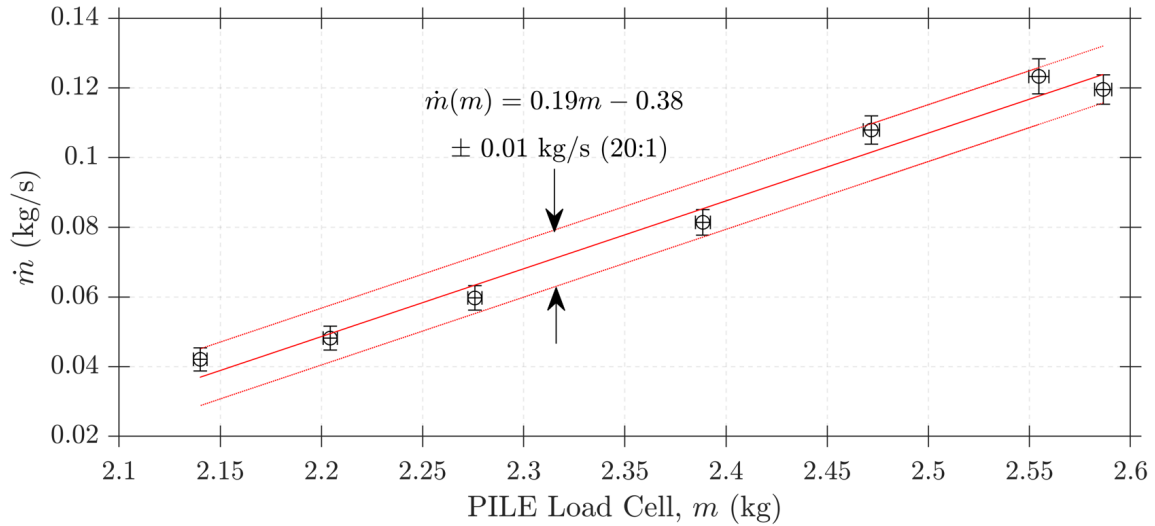


Figure 7. Experimental results for flow bin weight correlation with measured mass flow.

## 4. Alternative Commercial Flow Sensors

Microwave and acoustic sensing have been investigated and applied for particle flow characterization for over two decades and has had particular success in predicting mass flow rates with less than 10 % error in solid-gas flow regimes. However, they have not been successfully demonstrated in high-temperature environments ( $\geq 800$  °C). Microwave sensing techniques are completely non-intrusive to the particle flow and consists of an individual or array of antennas mounted on the exterior of the pipe or duct. With frequency-based analysis techniques, velocity information can be directly extracted from microwave signals. For example, in [7] and [8], Doppler signal analysis and spatial filtering velocimetry, respectively, were used to reconstruct particle velocity distributions and mass flow rates from an array of microwave measurements. Microwave tomography based on an array of antenna on the perimeter of pipes can also successfully reconstruct a 2D cross-sectional images that show the distribution of solids within mixed solid-gas flow inside of metal pipes [9].

Passive acoustic emission measurement techniques have long been applied in chemical engineering and powder technology processes [10]. Various frequency-based analysis methods have also been successful in extracting solid flow rate information from acoustic sensing assemblies. Although the acoustic sensing assembly can be completely non-intrusive such as in [11] and [12], it is often helpful to insert a wave guide into the flow to amplify the measurement as is demonstrated in [13].

## 5. Conclusion

The concept for continuous mass flow measurement of particles at high temperature is described in this paper. Simplified design and non-complex geometry contribute to the robustness and scalability of the device for measuring continuous mass flow under very harsh operating conditions. Due to the limited amount of hardware interfacing with high temperature flowing particle, the proposed concept have potential to be affordable at large scales. The initial experimental results that was obtained with the design described in earlier sections of this document indicate that a very stable signal can be obtained for a continuously resolution of varying mass flow rates. Gravimetric measurement would be required for calibration and characterization of the slotted flow bin, after which it can be installed in a particle flow stream for compact mass flow measurement. Influences from mechanical equipment vibration have been

identified and a source of uncertainty and signal noise that need to be addressed going forward. Design considerations for larger scale mass flow measurement and eventual utility scale applications will be covered in future work on this mass flow sensor.

## Data availability statement

Data from testing could be made available upon request by the team at the NSTTF. Raw test data will not readily available on an online platform.

## Author contributions

Hendrik Frederik Laubscher is the lead author, doing the engineering lead and supervised the student Samuel C. Hastings. Luke P. Kaden E. Plewe and McLaughlin is contributing with engineering consulting.

## Competing interests

The authors declare no competing interests.

## Funding

This project is funded by the Solar Energy Technologies Office from the U.S. Department of Energy.

## Acknowledgements

Sandia National Laboratories is a multimission laboratory managed and operated by National Technology & Engineering Solutions of Sandia, LLC, a wholly owned subsidiary of Honeywell International Inc., for the U.S. Department of Energy's National Nuclear Security Administration under contract DE-NA0003525. SAND2023-11279C.

## References

- [1] N. Schroeder and K. Albrecht, "Assessment of particle candidates for falling particle receiver applications through irradiance and thermal cycling," Jun. 2021. doi: <https://doi.org/10.1115/ES2021-62305>.
- [2] C. K. Ho et al., "SANDIA REPORT Particle Mass Flow Control for High-Temperature Concentrating Solar Receivers," no. May, 2018, [Online]. Available: [https://energy.sandia.gov/wp-content/uploads/dlm\\_uploads/2019/misc/08/G3P3/Fractal\\_particle\\_receiver\\_1506\\_SAND\\_v6\\_Final.pdf](https://energy.sandia.gov/wp-content/uploads/dlm_uploads/2019/misc/08/G3P3/Fractal_particle_receiver_1506_SAND_v6_Final.pdf)
- [3] A. Janda, I. Zúriguel, and D. Maza, "Flow rate of particles through apertures obtained from self-similar density and velocity profiles," *Phys. Rev. Lett.*, vol. 108, no. 24, 2012, doi: <https://doi.org/10.1103/PhysRevLett.108.248001>.
- [4] C. K. Ho et al., "Characterization of particle flow in a free-falling solar particle receiver," *J. Sol. Energy Eng. Trans. ASME*, vol. 139, no. 2, pp. 1–9, 2017, doi: <https://doi.org/10.1115/1.4035258>.
- [5] B. J. Harris, J. F. Davidson, and C. E. Davies, "Slot Flow Metering: Fundamental Investigations, Pilot Scale Tests and Industrial Prototype," *KONA Powder Part. J.*, vol. 10, no. 10, pp. 104–112, 1992, doi: <https://doi.org/10.14356/kona.1992015>.
- [6] Moffat, R. J. (1988). "Describing the Uncertainties in Experimental Results." *Experimental Thermal and Fluid Science* 1: 3-17

- [7] Zou, J., et al. (2020). "Mass flow rate measurement of bulk solids based on microwave tomography and microwave Doppler methods." *Powder Technology* 360: 112-119. <https://doi.org/10.1016/j.powtec.2019.09.087>.
- [8] Penirschke, A. and R. Jakoby (2008). "Microwave Mass Flow Detector for Particulate Solids Based on Spatial Filtering Velocimetry." *IEEE Transactions on Microwave Theory and Techniques* 56(12): 3193-3199. <https://www.doi.org/10.1109/tmtt.2008.2007142>.
- [9] Mallach, M., et al. (2017). "2D microwave tomography system for imaging of multi-phase flows in metal pipes." *Flow Measurement and Instrumentation* 53: 80-88. <https://doi.org/10.1016/j.flowmeasinst.2016.04.002>.
- [10] Boyd, J. W. R. and J. Varley. (2001). "The uses of passive measurement of acoustic emissions from chemical engineering processes." *Chemical Engineering Science* 56: 1749-1767. [https://doi.org/10.1016/S0009-2509\(00\)00540-6](https://doi.org/10.1016/S0009-2509(00)00540-6).
- [11] Ruiz-Carcel, C., et al. (2018). "Estimation of powder mass flow rate in a screw feeder using acoustic emissions." *Powder Technology* 336: 122-130. <https://doi.org/10.1016/j.powtec.2018.05.029>.
- [12] Jingdai, W., et al. (2010). "Characterization of flow regime transition and particle motion using acoustic emission measurement in a gas-solid fluidized bed." *AIChE Journal* 56: 1173-1183. <https://doi.org/10.1002/aic.12071>.
- [13] Zheng, G., et al. (2021). "Mass-Flow-Rate Measurement of Pneumatically Conveyed Particles Through Acoustic Emission Detection and Electrostatic Sensing." *IEEE Transactions on Instrumentation and Measurement* 70: 1-13. <https://doi.org/10.1109/TIM.2020.3039619>.